General Disclaimer

One or more of the Following Statements may affect this Document

- This document has been reproduced from the best copy furnished by the organizational source. It is being released in the interest of making available as much information as possible.

- This document may contain data, which exceeds the sheet parameters. It was furnished in this condition by the organizational source and is the best copy available.

- This document may contain tone-on-tone or color graphs, charts and/or pictures, which have been reproduced in black and white.

- This document is paginated as submitted by the original source.

- Portions of this document are not fully legible due to the historical nature of some of the material. However, it is the best reproduction available from the original submission.

DOE/NASA/12726-8
NASA TM-82607

NASA Preprototype Redox Storage System for a Photovoltaic Stand-Alone Application

Norman H. Hagedorn
National Aeronautics and Space Administration
Lewis Research Center

Work performed for
U.S. DEPARTMENT OF ENERGY
Conservation and Solar Energy
Division of Energy Storage Systems

Prepared for
Intersociety Energy Conversion Engineering Conference
sponsored by the American Society of Mechanical Engineers
Atlanta, Georgia, August 9-14, 1981

DOE/NASA/12726-8
NASA TM-82607

NASA Preprototype Redox Storage System for a Photovoltaic Stand-Alone Application

Norman H. Hagedorn
National Aeronautics and Space Administration
Lewis Research Center
Cleveland, Ohio 44135

Work performed for
U.S. DEPARTMENT OF ENERGY
Conservation and Solar Energy
Division of Energy Storage Systems
Washington, D.C. 20545
Under Interagency Agreement DE-AI04-80AL12726

Intersociety Energy Conversion Engineering Conference
sponsored by the American Society of Mechanical Engineers
Atlanta, Georgia, August 9-14, 1981

NASA PROPROTOTYPE REDOX STORAGE SYSTEM FOR A PHOTOVOLTAIC STAND-ALONE APPLICATION

Norman H. Hagedorn
National Aeronautics and Space Administration
Lewis Research Center
Cleveland, Ohio 44135

E-854

ABSTRACT

A 1-kW preprototype redox storage system has undergone characterization tests and has been operated as the storage device for a 5-kW (peak) photovoltaic array. The system is described and performance data are presented. Loss mechanisms are discussed and simple design changes leading to significant increases in efficiency are suggested. The effects on system performance of nonequilibrium between the predominant species of complexed chromic ion in the negative electrode reactant solution are indicated.

INTRODUCTION

The NASA Lewis Research Center redox systems concept embodies the use of the Fe^{+2}/Fe^{+3} and Cr^{+2}/Cr^{+3} redox couples, an anion-exchange membrane for reactant separation, and carbon felt electrodes. The pacing technologies for the development of the concept have been in the areas of the membrane and the chromium electrode. The membrane must have low resistivity yet form a barrier that selectively excludes the reactant cations. The chromium electrode must be catalytically active to the reduction and oxidation of the chromium ions but not to the chemical or electrochemical reduction of protons. During 1979 and early 1980 significant advances were made in both these critical areas. It then became feasible to develop and place on test a preprototype redox system of a size large enough to give meaningful insights into the requirements for subsequent designs. The preprototype system was designed to provide storage for a 5-kW (peak) array of solar photovoltaic cells at Lewis. This was deemed to be typical of the stand-alone applications in which early redox storage systems would most likely find use.

This paper describes the 1-kW preprototype redox storage system, its controls, and its optional configurations with regard to connection to the photovoltaic array. Performance data from several characterization tests are presented. Then the types and magnitudes of the various loss mechanisms associated with this particular system are discussed, including methods and estimates for the reduction of these losses in subsequent systems. Finally the results of operation of the complete, combined redox-photovoltaic system are presented and discussed.

Design Parameters

The nominal design specifications for the 1-kW preprototype redox system are presented in table I. For a more detailed discussion of system features and subsystem components, see reference 1. The 120-V dc voltage level was selected because of the large I^2R line losses that would occur at lower voltages. The decision to separate the single cells into four stacks was based partly on a consideration of shunt current losses (intrastack losses tend to increase with the square of the number of cells in a stack) and partly on the fact that 39-cell stacks represent a reasonable step up from the previous maximum number of cells in a stack, 14. The system capacity of 10 kWh (700 liters of each reactant) was an arbitrary choice based on convenience. For tests run to date the volume of reactants used was only about one-fourth of this design capacity. The depth-of-discharge range and the nominal current density were selected to avoid excessive pumping and cell IR losses. The cell size of 1/3 ft^2 active area was picked because the necessary equipment and material were already on hand.

The voltage level of 120 V dc presented a system design problem: Only 28-V dc pumps, controls, and instruments were readily available, and the lead times necessary to acquire 120-V equipment were not acceptable. It was therefore decided to use the 28-V equipment and to hard wire the 28-V pumps across a 24-cell section at the high-voltage end of the redox system (fig. 1). Because of the variation of the voltage across these cells as the state of charge of the system changes, the pumping rates will be greatest where low flow rates are acceptable, and lowest when high rates are needed. Either situation results in system inefficiencies. It was realized that the 28-V meter relays, flowmeters, and ampere-hour integrators could not tolerate the voltage changes inherent in direct connection to the redox stacks. It was therefore necessary to install a 120/28 dc-dc converter across the system 120-V dc bus. For the purpose of performing certain characterization tests, the option is provided to use external dc power supplies for the pumps and instrument controls. Obviously a system redesign would incorporate 120-V equipment and eliminate these costly and inefficient situations.

The redox system is designed so that, of the total of 156 single cells, 60 are separated into 10 six-cell trim packages. Through the use of meter relays, these trim packages are sequentially switched into or out of the load circuit to keep the bus voltage at 120 V dc. The trim packages and other working cells share common reactants at all times. Thus no part of the system is at a different state of charge from any other.

The photovoltaic array consists of twenty-two 120-V strings of solar cells that are also switched in and out to keep the array bus at 120 V dc, if possible, under existing load and insolation conditions. Trim cell switching is inhibited until all array strings are active, thus avoiding interactions between the two sets of controls. The array can be directly connected across the first 96 cells of the redox system (configuration 1) or directly across the system load in parallel with the active redox cells (configuration 2), as shown in figure 10.

Each of the four stacks in the system was checked out individually. As expected, the hydrogen evolution rates had become almost negligible. The average resistance of stack cells was about 12 mΩ, comparing well with laboratory results. However, the shunt current power losses, as indicated by the steady-state current ("taper current") attained while charging at a fixed voltage, were about twice as large as calculated. Most of this discrepancy subsequently has been shown to re-

sult from shunt paths unaccounted for in the mathematical model. These paths are effectively eliminated by using a plastic film to prevent the flowing fluids in the exit and inlet ports (fig. 2) from contacting the membranes. Table II shows, for five-cell stacks, the history of shunt current loss reduction as cells have been made to conform more closely to the model.

CHARACTERIZATION TESTS

The 1-kW preprototype system is shown in figure 3. The initial work, whose focus was to characterize the performance of the redox system, consisted of polarization tests, charge-discharge cycles, and performance-versus-flow-rate measurements (flow mapping). In these evaluations all 156 cells were active and system charging was done with a dc power supply. Also, for the reasons mentioned earlier, independent power supplies were used to power the pumps, the instruments, and the controls.

Figure 4 presents the polarization curves for the 156-cell redox system, taken at three different states of charge (SOC) and presented in terms of average cell voltage as a function of current density. The dip in the discharge curve for the lowest SOC occurred when the performance of the system's weaker cells (i.e., those cells receiving less than adequate flow) declined. The voltage of such cells tends to drop to near zero and then stabilize. The rise in the charging curve for the highest SOC was accompanied by the onset of an increased hydrogen evolution rate, which is typical for higher charging voltages. The linear segments of the discharge curves have a slope equivalent to 15 mΩ/cell, about 25 percent greater than measured when the stacks were tested individually. It was determined that this rise in cell resistance resulted from the inability of the test facility heating system to keep the reactant temperatures above 10° C in midwinter. The previous tests had been performed at a controlled 21° C. This temperature-induced increase of cell resistance results in a decrease in system energy efficiency. For actual storage applications the redox system would have to be protected from overcooling by burying or insulating it.

Charge-discharge cycles were performed at nominal current densities of 30, 38, and 45 mA/cm^2. The system, initially fully discharged, was charged at the desired rate until the charging voltage reached 187 V (1.20 V/cell), after which the current was allowed to taper off until a quasi-steady state of charge was attained. Discharge followed immediately and continued until complete discharge was attained. Typical data are shown in figure 5, in which the SOC, as indicated by the voltage of the open-circuit cell, is plotted against watt-hours of capacity, for both charge and discharge. For a cycle between the open-circuit voltage limits of 0.94 and 1.15 V, the energy efficiency was 56.7 percent. Similar data for ampere-hours of capacity show a coulombic efficiency of 83.9 percent. The contributors to these relatively low efficiencies were the greater-than-expected average cell resistance and the higher-than-calculated shunt current losses. As suggested in the preceding discussion, both of these loss mechanisms can be easily and significantly reduced.

Flow mapping tests were also performed. In these tests the reactant flow rates were varied during a charge-discharge cycle to determine what flows were necessary to sustain system performance at various states of charge. It was found that a flow rate three times greater than the stoichiometric requirement (i.e., the ideal minimum flow for a given current and SOC) is adequate to prevent any cells from falling to zero voltage during discharge or rising unacceptably during charge. Tests on single cells have shown that 1.5 times the stoichiometric flow rate is sufficient for good performance, so the fact that the 156-cell system requires twice this rate indicates that some cells are getting only about one-half their share of the total flow. This problem relates to the difficulty in maintaining assembly tolerances when producing many cells by hand.

Several additional characterization tests were performed but with the trim cell controllers operational. The first was a combined operation of the redox-photovoltaic system. Data from a typical run are presented in table III. The two systems were operated in configuration 1, in which the photovoltaic array is connected directly across the first 96 cells of the redox system. For the existing test conditions of load, redox state of charge, and solar insolation, the array was fully activated (all 22 solar cell strings functioning) but was unable to reach the 120-V dc operating level. Therefore two trim cell packages (12 cells) were automatically brought into the circuit to boost the array output voltage from 111.5 to 120.5 V for the load bus. Because of the relatively low redox system state of charge of 33 percent, the array was capable, even at its 111.5-V output voltage, of providing charge to the redox system through the 96-cell main stack. Thus the redox system was expending 167 W through its trim cells to boost the array power to the load by 9 V and was at the same time accepting 1170 W of charge. During these tests the pumps, instruments, and controls were still being powered by separate power supplies. All controls and switching devices operated normally.

Another set of characterization tests was made to determine the system response to transient loads such as the current surges required for motor starting. For the first of these tests the redox system and the photovoltaic array were both operational. Figure 6 shows the time variation of the load current and the sharing of that current by the array and the redox system when the starting of a 250-W, 120-V dc motor was superimposed upon a steady-state resistive load of 1 kW. The magnitude of the load current spike was 20 A. The redox system absorbed 95 percent of this surge, going from a steady-state charge acceptance of 16.5 A to a peak discharge rate of 2.5 A.

The final transient test was performed with a 1-kW, 120-V dc vacuum pump motor equipped with a starting resistor. The array was not in operation, and the redox system was at 55 percent state of charge. The data recorder traces for the load current and the terminal voltage are shown in figure 7. The shape and ripples of the traces are related to the action of the resistive starter and to the pump starting characteristics. During the first 100 ms of the transient, six trim cell packages (36 cells) were activated. Although the peak load was greater than 2100 W, there was no tendency toward stalling of the motor, and the redox system returned to its nominal operating voltage in 500 ms.

Finally the redox system was charged to approximately 80 percent SOC and then allowed to discharge at a 10-A rate (pump and controls externally powered). The system voltage and the open-circuit cell voltage are plotted together in figure 8, which shows the action of the trim cells maintaining system voltage as the state of charge decreases. Not until all cells are active does system output start to decay.

EFFICIENCY LOSS MECHANISMS

Inefficiencies associated with the preprototype, 1-kW system can be significantly reduced. Table IV presents the measured nominal losses for the 1-kW system. The pumping loss relates to the maximum design requirement for three times the stoichiometric flow rate based on the design gross current density and the

maximum design depth of discharge (80 percent). Better control over cell assembly tolerances would assure that all cells receive their proportionate share of the total flow and would thus permit operation closer to the 1.5 stoichiometric flow multiple shown to be sufficient for single cells. Since pump power varies directly with nearly the cube of the flow rate, this flow rate reduction would have a significant effect. Pumps having an electric-to-hydraulic efficiency greater than the present 15 percent also would greatly reduce pumping losses. However, for very small systems such as this, low pump efficiency is a fact of life unless the pumps are designed for the specific application. Finally, use of an efficient pump speed control and solid-state logic devices would permit varying the pump speed as a function of the system state of charge instead of operating at the fixed high speed required for the worst-case situation. Over a complete cycle this capability would reduce the total energy required for pumping by an estimated 50 percent.

As mentioned earlier a simple cell design change already implemented and proven in laboratory stacks can be expected to reduce the intrastack shunt losses by about 50 percent. In addition, operation at lower flow rates will permit the narrowing of the flow port slots in each cell at the expense of only modest pumping losses. Within certain limits the intrastack shunt losses are directly proportional to these flow port widths (resistances). In like manner, interstack losses can be reduced by lengthening the piping between stacks or reducing the piping diameter. Finally a computational process can be used to determine the number of stacks, the number of cells per stack, and the size of the piping connecting stacks to minimize the sum of intra- and interstack shunt losses and pumping power.

The power requirement indicated in table IV for instrumentation and controls is specifically for the meter relays and associated contactors for the trim cell control and for several integrating ampere-hour meters. The latter, being research devices, should not have their energy needs charged to the system. The former can be replaced by solid-state switching devices, and this will considerably reduce their power demands. Finally, although not tabulated in table IV, the I^2R losses could be reduced 20 percent merely by raising the system temperature 10° C, as discussed earlier.

It should be noted that the pump and shunt losses presented in table IV are maximum values. If the pump speeds were varied continuously in order to keep the flow rates at a constant multiple of the instantaneous stoichiometric flow rates as the system SOC changed, the average pump power during a complete cycle would be much less than the indicated value. Similarly the listed shunt loss rate is for charging at the maximum rate (i.e., when the system voltage is at its highest). Since the shunt losses tend to vary directly with the second to third power of the system voltage, the integrated average shunt loss during a cycle would be considerably reduced.

OPERATION OF COMBINED REDOX-PHOTOVOLTAIC SYSTEM

Upon completion of the characterization tests discussed in a preceding section, the intent was to couple the redox storage system and the photovoltaic array; to power the system pumps, controls, and instrumentation internally; and to begin operation in a mode that would typify a stand-alone application. The purpose of such operation was to determine storage system efficiency and capacity retention in this application. However, neither of these characteristics can be simply evaluated if the chromic ion species are not in equilibrium.

It has been determined that the chromic ion exists in two complexed forms, the penta aqua chloro ("penta") and the hexa aqua ("hexa"). The penta accepts a charge readily; the hexa, with difficulty. For a given state of charge, the greater the hexa content of the chromium solution, the greater is the open-circuit voltage of a redox cell. This causes the hysteresis in the open-circuit-voltage-versus-SOC curves of figure 9. At equilibrium in the discharged (chromic) state the penta and hexa concentrations are about equal, but equilibrium is reached very slowly. At equilibrium in the charged (chromous) state the penta form predominates, and equilibrium between the two species occurs rapidly.

In principle the measurement of system efficiency is quite straightforward. In order to determine system efficiency over some period of time, it is necessary to know not only the energy from the array and the energy to the load, but also the amount of energy stored. With the chromic ion species in equilibrium there exists a monotonic relationship between open-circuit voltage and system state of charge, and the change in energy stored can be easily calculated from the measured open-circuit voltages at the beginning and end of the subject time period. However, since the open-circuit voltage at any given SOC is a function of the chromium solution composition, the magnitudes of changes in the SOC are not well defined when the chromic species are not in equilibrium, and the efficiency is then difficult to determine.

The same situation affects the measurement of the change in system capacity with time. Capacity retention can be determined by charging from one specified value of open-circuit voltage to another and measuring the amount of charge required. However, the initial composition of the chromium solution depends on the recent operating history of the system, and this initial composition determines the amount of charge needed to reach the target open-circuit voltage. The effects of imbalance of the chromic ion species on system operating characteristics are very application dependent. They are affected by such factors as the ratio of total cell area to reactant volume, charge-discharge rates, and the shape of the duty cycle. Operationally some of the ramifications of this system characteristic are (1) that extended periods in the discharged state should be avoided and (2) that the charge rate should be low enough relative to the theoretical capacity to permit hexa-penta equilibruim to be maintained. Research is now under way to quantify this further and to uncover materials that will catalyze either the penta-hexa equilibrium reaction or the direct reduction of the hexa species.

The last test performed to date was a brief comparison of the two optional connections of the array to the redox system. As shown in figure 10, in configuration 1 the array is hard wired across a 96-cell group of redox cells, in configuration 2 it is directly connected to the load. In table V the comparison of configurations is made at two indicated states of charge. It can be seen that the charging power from the array is greater when it is allowed to work into a lower voltage (i.e., configuration 1) so that it operates closer to its peak power point. Therefore for an application in which the main purpose of the array is to charge the redox system for later use, perhaps at night, configuration 1 would be the choice. On the other hand, if the load and array are operational at the same time, configuration 2 would minimize the amount of load energy that had to go through the less efficient electrochemical charge-discharge sequence. Thus the choice will depend on the application and be decided by economics.

CONCLUDING REMARKS

Significant progress has been made over the last 3 years in advancing the redox technology. Incorporating the most recent developments in membrane and electrode technology into a complete, fully integrated storage system and evaluating the system under realistic conditions have added greatly to the credibility of the redox storage system concept. Experience gained from operation of the 1-kW preprototype system is also of value in directing the continuing development effort.

The 1-kW redox preprototype system, although operational for only a short time, has already provided much valuable information. Control concepts have been shown to be valid and trouble free. Some insight has been gained into interactions at the mutual interfaces of the redox system, the photovoltaic array, the load, and the control devices. Quantitative measurements of loss mechanisms have given direction for stack and system design changes to minimize these losses. Operating characteristics of the system, especially insofar as they relate to the equilibria of species in the chromium solution, have been partially quantified. The response of the system to transient loads has been measured, and some of the criteria for the choice of system configuration have been developed.

Significant improvements in system efficiency can be achieved without any technological breakthroughs. A system larger than the 1-kW preprototype would permit larger, more efficient pumps to be used. Varying pump speed to maintain a constant multiple of the stoichiometric flow requirement would further reduce pumping energy by as much as 50 percent. For larger cells shunt losses would become a smaller fraction of system power. A recent verified improvement in cell design would make significant further reductions in shunt losses. The fact that membrane resistance rises with decreasing temperature would require passive thermal management in the design of a larger system. This would reduce the I^2R losses observed during operation of the 1-kW preprototype system.

Additional efficiency improvements will occur as the state of technology advances: Expected reductions in membrane resistivity will lower still further the system I^2R losses. Improving the kinetics of reaction and/or equilibration for the various species of complexed chromic ion will also enhance system performance.

REFERENCE

1. Thaller, Lawrence H.: Redox Flow Cell Energy Storage Systems. NASA TM-79143, 1979, DOE/NASA/1002-79/3.

TABLE I. - REDOX SYSTEM DESIGN PARAMETERS

Gross power, W	1260
Nominal net power, W	1000
Voltage, V dc	120±5%
Number of stacks	4
Number of cells per stack	39
Number of trim packages (6 cells each)	10
Depth-of-discharge range, percent	80-20
Reactant volume (each), liters (U.S. gallons)	700 (186)
Reactant energy density (end of life), Wh/liter	14.5
Cell active area, cm^2	320
Nominal current density, mA/cm^2	30
Reactants	1M/liter $FeCl_3$, 2N HCl
	1M/liter $CrCl_2$, 2N HCl
Reactant flow rates per cell (nominal), cm^3/min	100-150
Parasitic losses, W:	
Pumps (15 percent pump efficiency)	120
Shunt power	120
Number of rebalance cells	5
Number of charge-indicator cells	1

TABLE II. - REDUCTION OF SHUNT CURRENT LOSS (TAPER CURRENT) BY CELL DESIGN CHANGES

[Five-cell stacks, 1.20 V/cell.]

Configuration	Taper current, mA
Original	2000
Bipolar plate manifold holes insulated from fluids	140
Membrane manifold holes insulated from fluids	28
Membranes insulated from fluids in exit and inlet port	12
Mathematical model	7

TABLE III. - PERFORMANCE DATA, COMBINED REDOX/PHOTOVOLTAIC SYSTEM

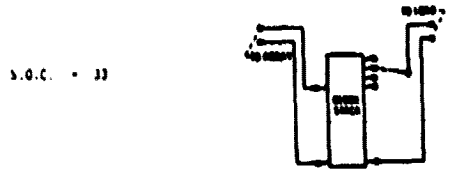

	CONFIGURATION 1
INSOLATION, MW/CM^2	78.2
TRIM CELLS ACTIVE	12.0
ARRAY VOLTAGE, VOLTS	111.5
ARRAY CURRENT, AMPS	29.1
LOAD VOLTAGE, VOLTS	120.5
LOAD CURRENT, AMPS	18.6
MAIN STACK VOLTAGE, VOLTS	111.5
MAIN STACK CURRENT, AMPS	5 (CHARGE)
TRIM CELL VOLTAGE, VOLTS	.0
TRIM CELL CURRENT, AMPS	18.6 (DISCHARGE)
DISCHARGE POWER (TRIM CELLS), WATTS	167.0
ARRAY POWER, WATTS	3245.0
LOAD POWER, WATTS	2241
CHARGE POWER, WATTS	1171

TABLE IV. - TABULATION OF PARASITIC LOSSES FOR THE PREPROTOTYPE 1-kW REDOX STORAGE SYSTEM

	Measured	Design estimate
	Loss, W	
Pumps	120 (max.)	120
Shunt currents	230 (max.)	120
Instruments and controls	100	---

TABLE V. - EFFECT OF SYSTEM CONFIGURATION ON CHARGING RATE

	Configuration 1		Configuration 2	
	State of charge, percent			
	35	44	35	44
Number of trim cells active	12	12	12	12
Array voltage, V	110.0	113.5	121.5	125.4
Charging current, A	6.6	7.37	5.6	6.39
Charging power, W	726	836	680	801

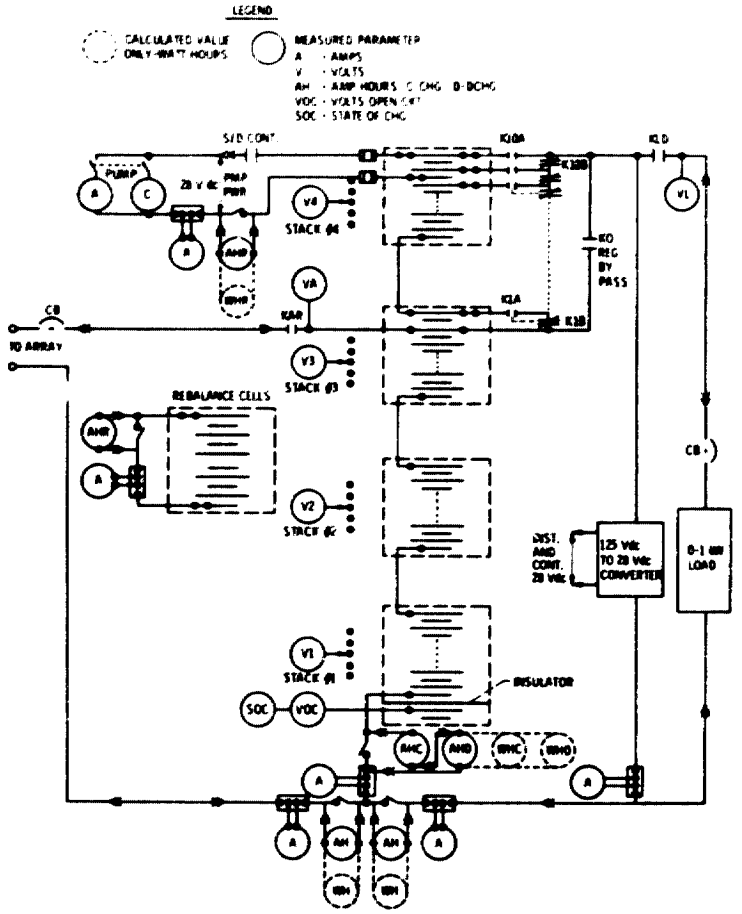

Figure 1. - Electrical diagram of the 1.0 kilowatt system showing instrumentation and data acquisition points.

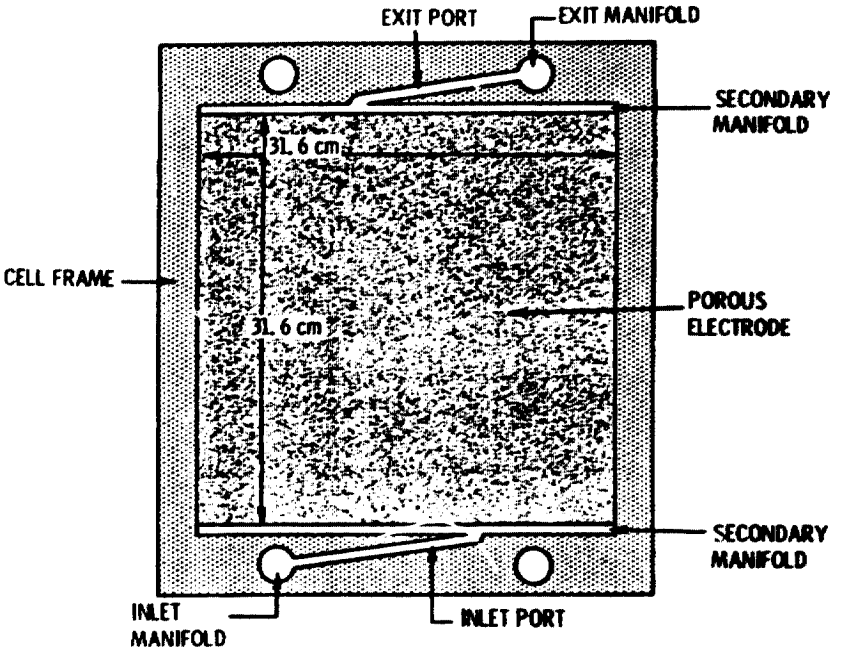

Figure 2. - Planform of typical NASA-Lewis Redox cell -- 1000 cm^2 active area (cell size for 1 kW system is 320 cm^2 active area).

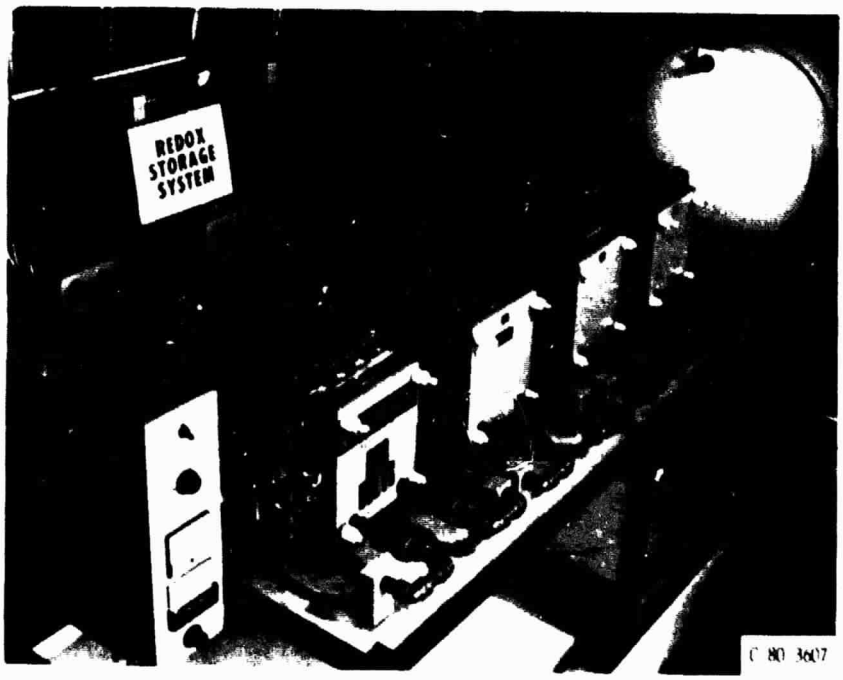

Figure 3. - The 1-kilowatt preprototype redox storage system.

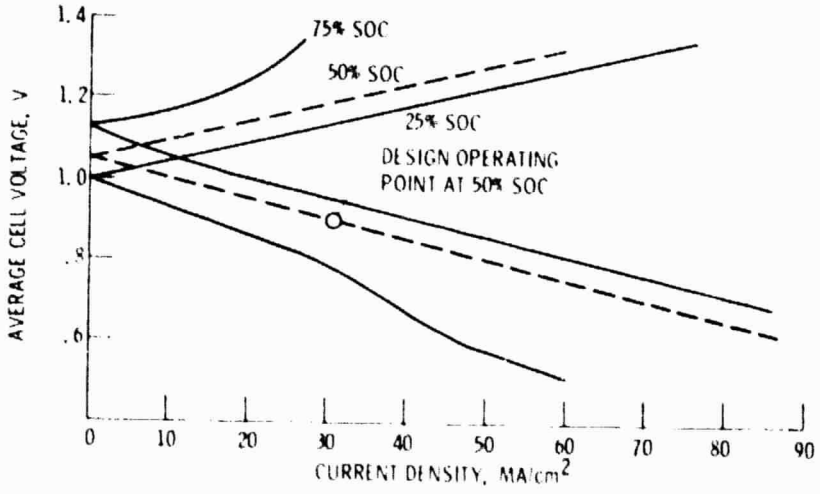

Figure 4. - Polarization curves, charge and discharge, for the 1 kW Redox storage system at three different states of charge.

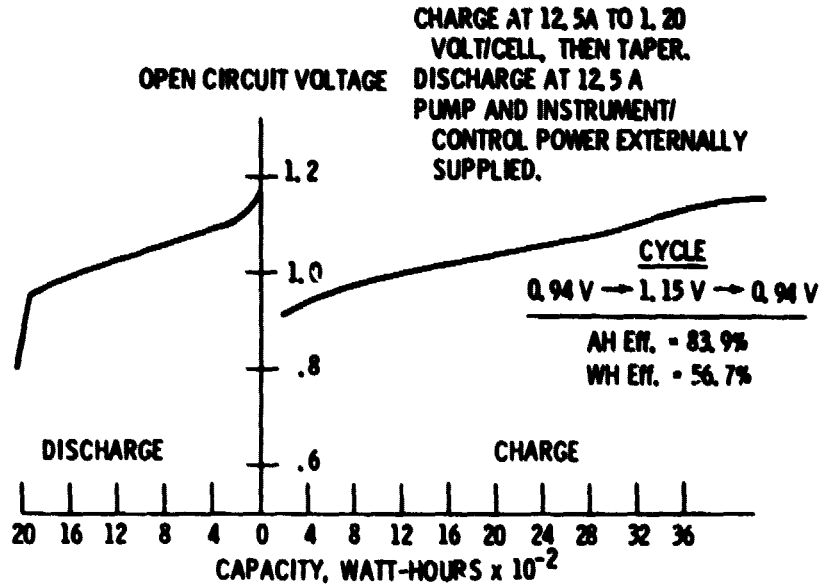

Figure 5. - Charge-discharge cycle for 1 kW Redox storage system: Capacity vs. Open Circuit Voltage.

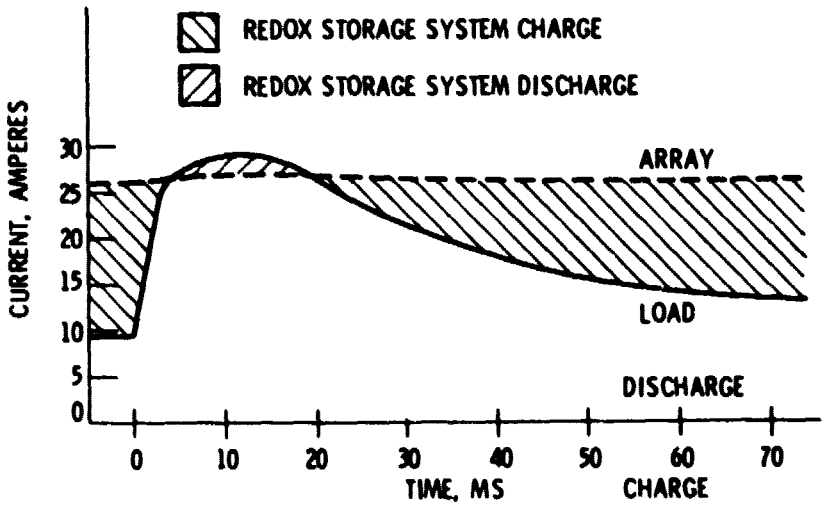

Figure 6. - Load sharing between Redox storage system and photovoltaic array during a 250-watt motor starting transient superimposed on a 1 kW steady-state load (28% state-of-charge).

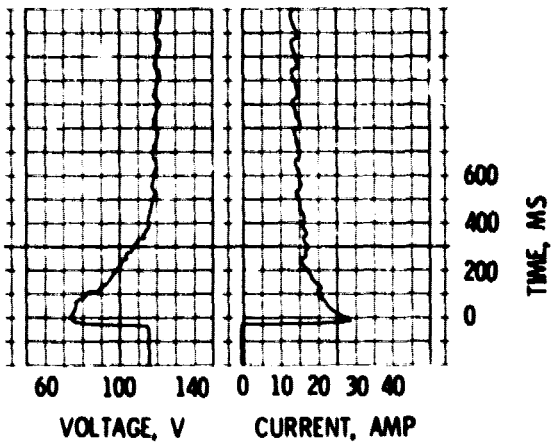

Figure 7. - Starting transients, voltage and current, for 1 kW, 120 VDC pump motor. Redox system at 55% state-of-charge.

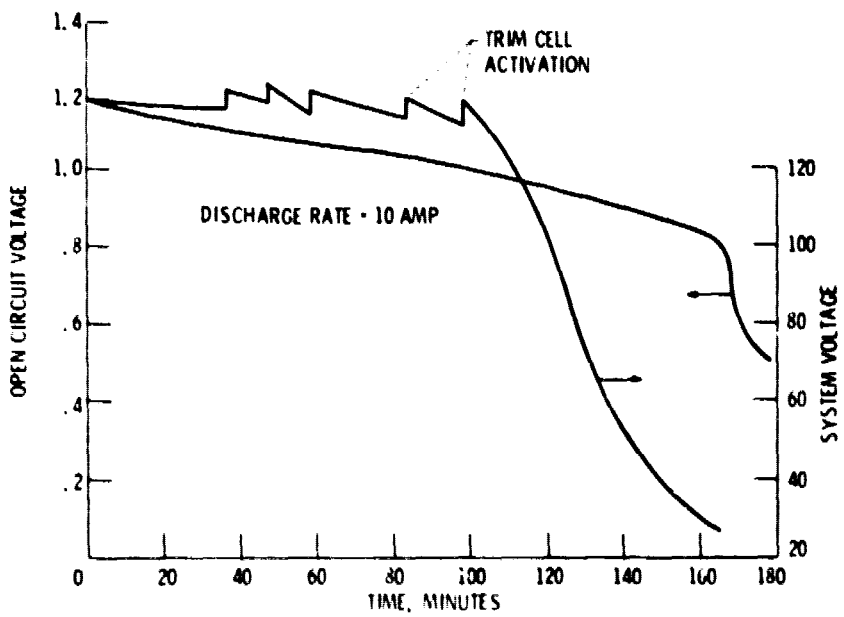

Figure 8. - System voltage and open-circuit cell voltage during discharge, showing effect of trim cell operation.

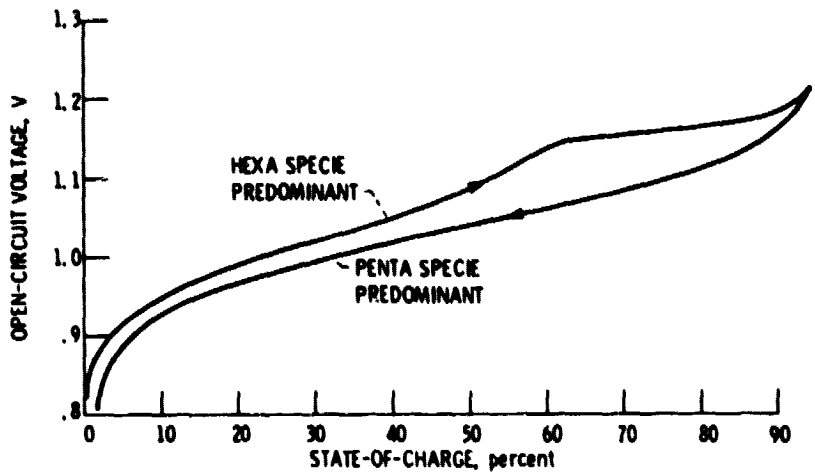

Figure 9. - Open circuit voltage as a function of state-of-charge, during charge and discharge.

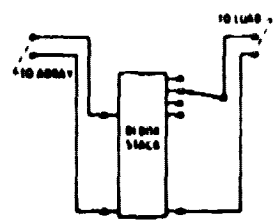

(a) Configuration 1. Array connected across 96-cell section of Redox system.

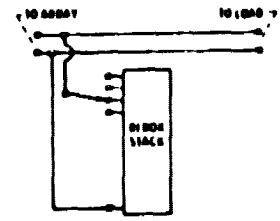

(b) Configuration 2. Array connected directly to load, in parallel with Redox system.

Figure 10. - Optional combinations of the Redox system and the photovoltaic array.